Graphene Point Defects: An Application of Deep Learning to MD Simulation

Zahra Wray[a,b], Pablo Piaggi[c], Roberto Car[c,d]
[a] *Department of Chemistry and Biochemistry, Hunter College, The City University of New York, 695 Park Ave, New York, NY 10065*
[b] *Department of Chemistry and Biochemistry, Macaulay Honors College, The City University of New York, 35 W 67th St, New York, NY 10023*
[c] *Department of Chemistry, Princeton University, Princeton, NJ 08544*
[d] *Department of Physics, Princeton University, Princeton, NJ 08544*

Abstract
Graphene's impressive mechanical, chemical, electronic, and magnetic properties enable applications in a variety of fields. Point defects – atomic-scale imperfections in an otherwise uniform lattice structure – can influence these unique properties. Advancements in machine learning methods recently allowed for the execution of calculations with (reasonably) high accuracy and efficiency by neural networks. As such, the incorporation of machine learning training (to computational methods and MD sim.) could yield promising results for future investigations into materials such as graphene.

1. Introduction

Graphene is a one-atom thick, two-dimensional monolayer of sp^2 hybridized carbon atoms arranged in a honeycomb (hexagonal) lattice.[1] Its multitude of remarkable properties, including: phenomenal mechanical strength, large specific surface area, high electron mobility, amplified thermal conductivity, and acute optical transparency, enable applications across a wide range of fields (sensors, biomedicals, materials, microelectronics, etc.).[2,3]

Point defects, atomic-scale imperfects in otherwise perfectly uniform crystal lattices, either occur naturally or are intentionally inserted during the graphene growth process.[4] For instance, (single) vacancy defects – in which a single carbon atom is missing from the atomic structure – and Stone-Wales defects – (a type of topological defect) in which a pair of carbon atoms is rotated, resulting in adjacent pairs of pentagonal and heptagonal rings, surrounded by the iconic honeycomb lattice. Point defects are of

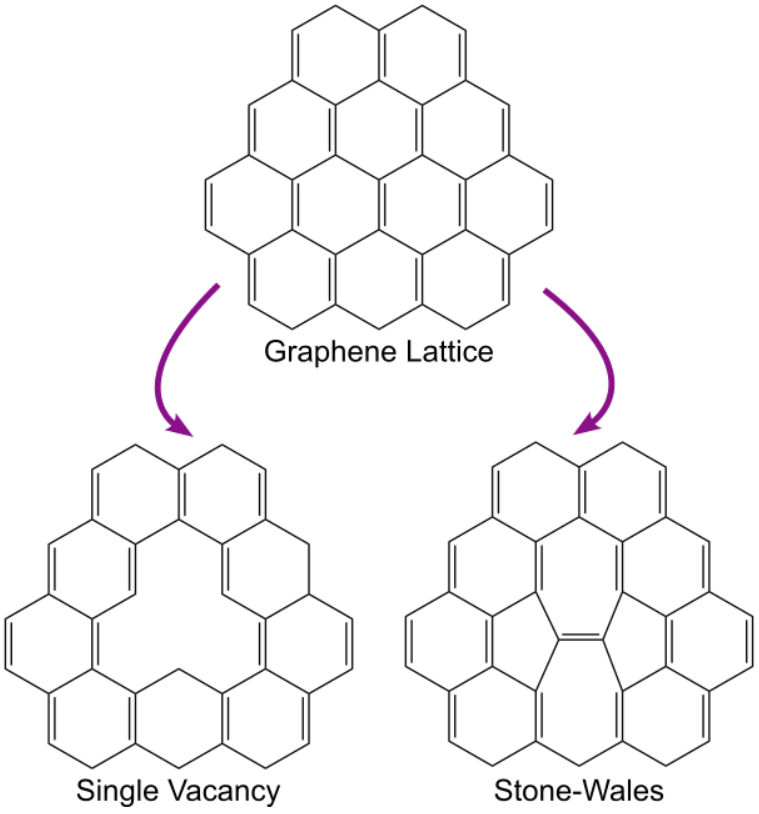


Fig. 1. Representative structures of graphene's hexagonal (honeycomb) lattice, with and without the implementation of the point defects (single vacancy and Stone-Wales) discussed in the text.

particular interest because they can influence the chemical, electronic, magnetic, and mechanical properties of graphene.[5]

Graphene's potential to revolutionize entire disciplines has continuously spurred scientific interest over the past several decades.[6] Additionally, recent developments in machine learning methods have allowed for the execution of MD simulations with relatively high accuracy, comparable to that of DFT, and efficiency which parallels empirical potential-based molecular dynamics.[7] As such, the application of neural network training to molecular dynamics simulations could have promising implementations for the investigation into graphene's properties.

2. Methods

Pseudopotentials for the bulk graphene system were sourced from D. R. Hamann, *Phys. Rev. B*. 88, 085117.[8] Input files for the bulk graphene structural optimization (vc-relax) calculations were generated using ASE (Atomic Simulation Environment) for a graphene system containing 60 carbon atoms. These input files were modified for use in the subsequent optimization calculations of the graphene system containing a single vacancy defect.

Using Quantum ESPRESSO, electronic-structure calculations (based on Density Functional Theory, DFT) were performed on the graphene system.[9,10] Molecular dynamics simulations (and calculations) were facilitated by Deep Learning (DeePMD-kit) neural networks (via. LAMMPS).[7,11,12] Ovito (Open Visualization Tool) was utilized for visualization.[13]

Density of states (DOS) datafiles were compiled from the output files of successive scf, nscf (non-self-consistent field) and dos calculations. Band structure datafiles were compiled from the output files of bands calculations. The fermi energy was corrected using the output of the nscf calculation. Structural optimization calculations were utilized for a convergence test. A set of vc-relax calculations were performed with varying wavefunction cutoff (ecutwfc) values. The convergence test yielded an optimal wavefunction cutoff of 70 Ry, which was used in the following scf calculations.

Machine learning preparation protocol: (1) A set of perturbed self-consistent field (scf) calculation input files were generated from the output of a structural optimization (vc-relax) calculation (or from the dump files of previous DPMD, LAMMPS calculations). Within each scf-input file, the atomic positions of the bulk graphene system were randomly displaced (maximum displacement = 0.01 Å); (2) Scf calculations were performed for each iterated system. Atomic structures (coordinates, types), potential energy, and atomic forces were parsed from the scf-outputs and converted to NumPy formats; (3) Training was commenced for the DeePMD neural network with 1,000,000 training steps. Trained models were subsequently frozen and compressed to optimize interference performance time. Several neural networks were trained with varying 'seeds' (used to generate random numbers when initializing the model parameters) to obtain deviation data; DPMD calculations were performed with 100,000 steps (nvt. at 300K). (RMS) error (of energy, forces) analysis and visualization of the system were performed. During the active learning protocol, configurations were extracted from the DPMD simulations, along with ab-initio information, and the protocol was repeated to refine the trained model.

3. Results

Structural optimization calculations (vc-relax) were executed on the graphene system (atomic positions and lattice constants were allowed to vary) and utilized to perform a convergence test – which yielded an optimized wavefunction cutoff of 70 Ry. The lattice constant for each wavefunction cutoff (ecutwfc) value was calculated from the unit cell's parameters. The lattice constant was plotted against the wavefunction cutoff. The lattice constant for the graphene system at 70 Ry was calculated to be 2.461 Å, which corresponds to the literature value of 2.46 Å.[14]

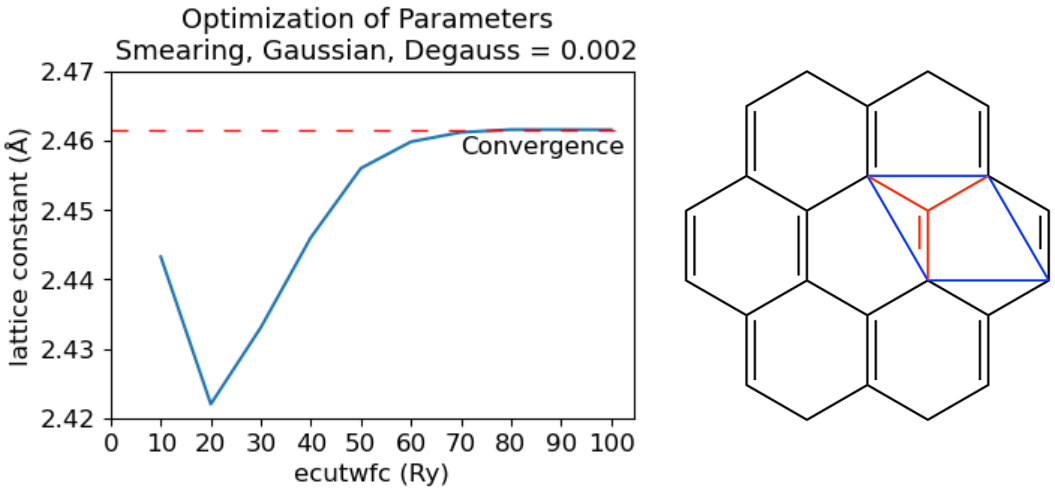


Fig. 2. (Left) Lattice constant convergence plot (lattice constant [Å] vs. ecutwfc [Ry]), (Right) Representative structure of the graphene structure, the unit cell is highlighted.

Graphene's band structure confirms its semi-metal properties – the conduction and valence bands meet at the symmetry point K, where there is no band gap. This directly corresponds to the Density of States plot (as shown by the fermi energy), where Energy (in eV) and DOS are equal to 0.

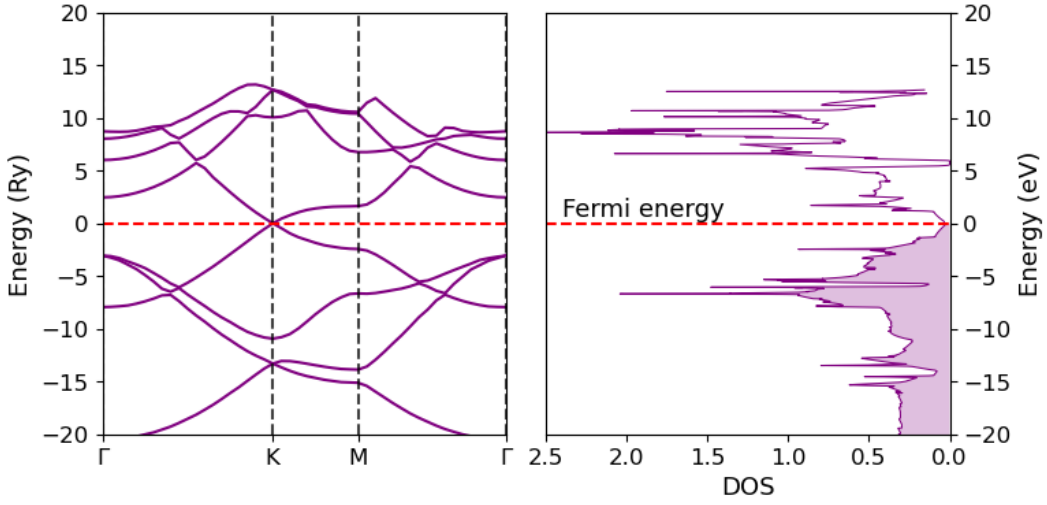


Fig. 3. (Left) Graphene band structure and (Right) Density of States plot (Energy [eV] vs. DOS). Fermi energy = 1.4052. Points Γ correspond to the centers of the Brillouin zone, while Point K corresponds to the corners of the Brillouin zone, and Point M corresponds to the centers of the edges of the Brillouin zone.

Error analysis was performed for the bulk graphene system. Root mean square (RMS) errors converged below 10^{-2} eV/atom (for error of energy) and 10^{-1} eV/Å (for error of forces). Low values for the RMS indicated that the model fitted the data well and produces precise predictions. Deviation data (of forces, virial) was generated from the DPMD simulation computed with respect to four total models. The average deviation for the DPMD simulation remained below 0.050 ev/Å (a considerably tiny value), which demonstrates excellent consistency of the force predictions of multiple models (good agreement between models with varied 'seeds').

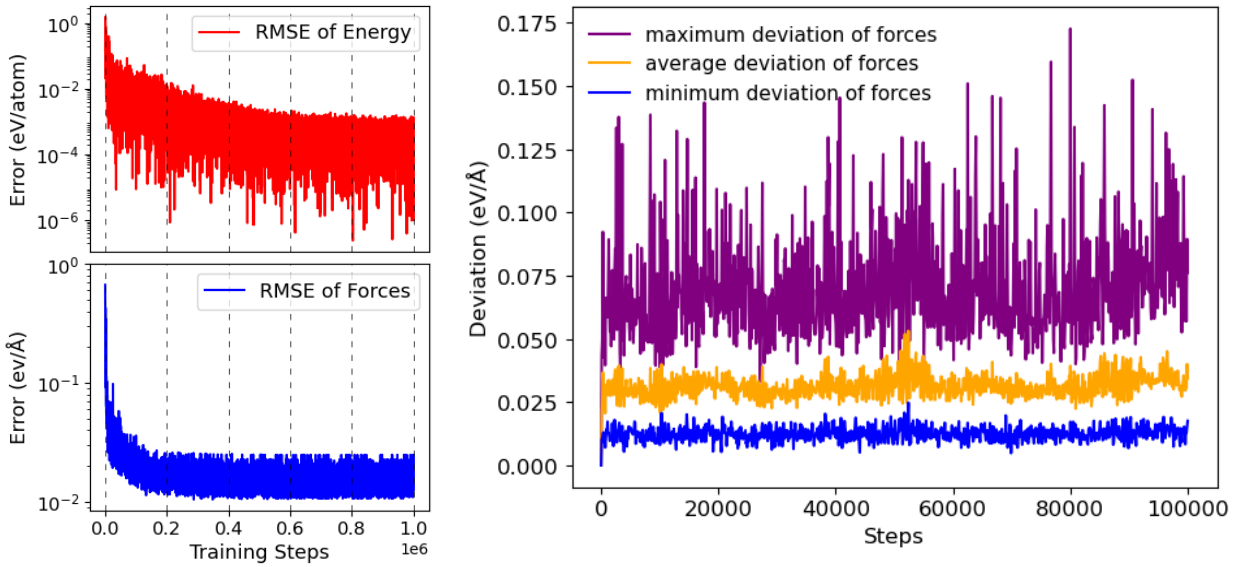


Fig. 4. (Left) Root Mean Square Error (RMSE) of a perturbed graphene sheet, trained for 1,000,000 steps – as given by, $RMSE = \left\langle \left(X_{pred} - X_{true}\right)^2 \right\rangle^{1/2}$, for a quantity, X, with predictions, X_{pred}, and ground truth, X_{true}. RMSE of energy is normalized by the number of atoms in the system. (Right) Deviations taken from a DPMD simulation relating to four trained models (a single DP model is used for representation of the potential energy surface), for 100,000 steps.

Parity plots show that the experimental values (DPMD forces/energy) corroborate with the predicted values (DFT forces/energy). Likewise, the distribution of errors for forces is represented by a *normal* distribution. The distribution of errors for energy displays a more abnormal (deviation from normal gaussian-like) distribution. A potential cause could be the exclusion of (900) additional scf-calculations from the parsed atomic structures, potential energies, and atomic forces, after the refinement of the model (during active learning).

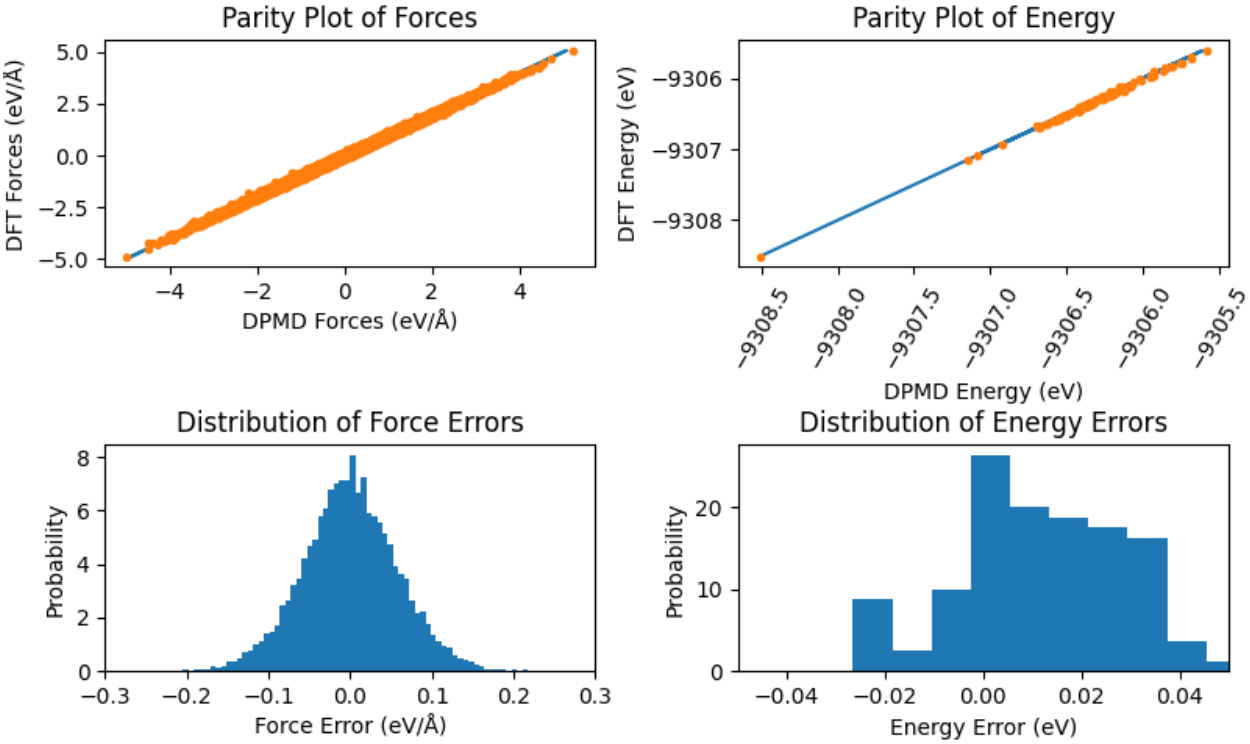


Fig. 5. (Top, Left) Parity Plot of Forces (DFT Forces [ev/Å] vs. DPMD Forces [ev/Å]), (Top, Right) Parity Plot of Energy (DFT Energy [ev] vs. DPMD Energy [eV]), (Bottom, Left) Distribution of Force Errors (Probability vs Force Error [ev/Å]), (Bottom, Right) Distribution of Energy Errors (Probability vs. Energy Error [ev/Å]).

The experimentally obtained phonon dispersion relation of graphene has excellent agreement with predictions calculated with DFT. The phonon dispersion possesses three optical branches and three acoustic branches, as expected.

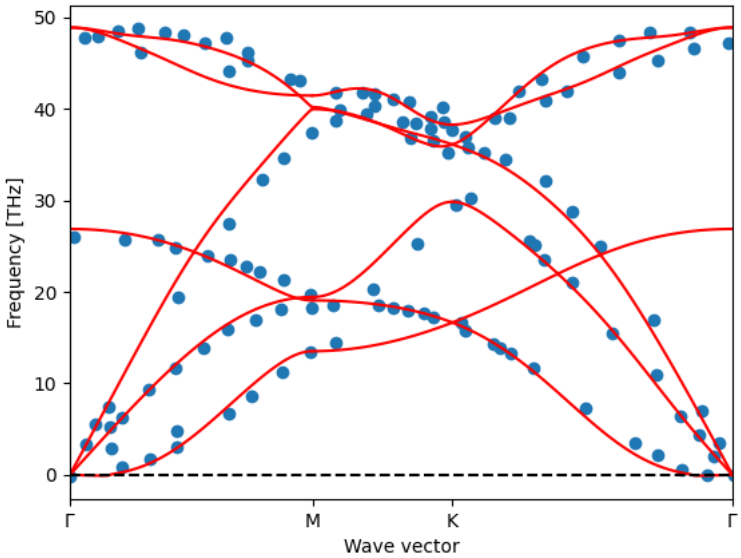


Fig. 6. Phonon dispersion relation of graphene (along the high symmetry lines of the hexagonal lattice). Points Γ correspond to the centers of the Brillouin zone, while Point K corresponds to the corners of the Brillouin zone, and Point M corresponds to the centers of the edges of the Brillouin zone.

4. Conclusions

To conclude, computational molecular dynamics methods and DFT calculations were employed to study the electronic structure of graphene. Machine learning models were trained based on DFT energies and forces. The trained model was capable of reproducing (from principle) many experimental properties of graphene, such as the lattice constant and the phonon dispersion relation. Neural network training could have promising implementations in the investigation of graphene's properties – potentially allowing for the realization of a greater range of applications.

Acknowledgements

I would like to thank Dr. Roberto Car and Dr. Pablo Piaggi, as well as the postdocs and graduate students of the Chemistry in Solutions and at Interfaces (CSI) Center of Princeton University, who provided technical assistance and additional guidance during the project's duration. The simulations presented in this report were performed on computational resources managed and supported by Princeton Research Computing, a consortium of groups including the Princeton Institute for Computational Science and Engineering (PICSciE) and the Office of Information Technology's High Performance Computing Center at Princeton University.

References

[1] Allen, M. J.; Tung, V. C.; Kaner R. B. Honeycomb Carbon: A Review of Graphene. *Chem. Rev.* **2010,** *110* (1), 132-145**.** DOI:10.1021/cr900070d

[2] Urade, A.R.; Lahiri, I.; Suresh, K. S. Graphene Properties, Synthesis and Applications: A Review. *JOM (1989).* **2023**, *75* (3), 614-630. DOI:10.1007/s11837-022-05505-8

[3] Tiwari, S. K.; Sahoo S.; Wang N.; Huczko A. Graphene research and their outputs: Status and prospect, *J. Sci.: Adv. Mater. Devices.* **2020**, *5* (1), 10-29. DOI:10.1016/j.jsamd.2020.01.006

[4] Fowler, W. B. Point defects. In *Reference Module in Materials Science and Materials Engineering.* Elsevier, **2022**. DOI: 10.1016/B978-0-323-90800-9.00085-8

[5] Tian, W.; Li, W.; Yu, W.; Liu, X. A Review on Lattice Defects in Graphene: Types, Generation, Effects and Regulation. *Micromachines (Basel).* **2017**, *8* (5), 163. DOI:10.3390/mi8050163

[6] Taghioskoui, M. Trends in graphene research. *Mater Today*. **2009**, *12* (10) 34-37. DOI: 10.1016/S1369-7021(09)70274-3.

[7] Wang, H.; Zhang, L.; Han, J.; Weinan, E. W. DeePMD-kit: A deep learning package for many-body potential energy representation and molecular dynamics. *Comput. Phys. Commun.* **2018**, *228*, 178-184. DOI:10.1016/j.cpc.2018.03.016.

[8] Hamann, D. R. Optimized norm-conserving Vanderbilt pseudo-potentials. *Phys. Rev. B: Condens. Matter Mater. Phys.* **2013**, 88.

[9] Giannozzi, P.; Baroni, S.; Bonini, N.; Calandra, M,; Car, R.; Cavazzoni, C.; Ceresoli, D.;
Chiarotti, G. L.; Cococcioni, M.; Dabo, I.; Dal Corso, A.; de Gironcoli S.; Fabris, S.; Fratesi, G.; Gebauer, R.; Gerstmann, U.; Gougoussis, C.; Kokalj, A.; Lazzeri, M.; Martin-Samos, L.; Marzari, N.; Mauri, F.; Mazzarello, R.; Paolini, S.; Pasquarello, A.; Paulatto, L.; Sbraccia, C.; Scandolo, S.; Sclauzero, G.; Seitsonen, A. P.; Smogunov, A.; Umari, P.; Wentzcovitch, R. M. QUANTUM ESPRESSO: a modular and open-source software project for quantum simulations of materials. *J Phys Condens Matter.* **2009**, *21* (39). DOI: 10.1088/0953-8984/21/39/395502.

[10] Giannozzi, P.; Andreussi, O.; Brumme, T.; Bunau, O.; Buongiorno Nardelli, M.; Calandra, M.; Car, R.; Cavazzoni, C.; Ceresoli, D.; Cococcioni, M.; Colonna, N.; Carnimeo, I.; Dal Corso, A.; de Gironcoli, S.; Delugas, P.; DiStasio, R. A.; Jr, Ferretti, A.; Floris, A.; Fratesi, G.; Fugallo, G.; Gebauer, R.; Gerstmann, U.; Giustino, F.; Gorni, T.; Jia, J.; Kawamura, M.; Ko, H. Y.; Kokalj, A.; Küçükbenli, E.; Lazzeri, M.; Marsili, M.; Marzari, N.; Mauri, F.; Nguyen, N. L.; Nguyen, H. V.; Otero-de-la-Roza, A.; Paulatto, L.;

Poncé, S.; Rocca, D.; Sabatini, R.; Santra, B.; Schlipf, M.; Seitsonen, A. P.; Smogunov, A.; Timrov, I.; Thonhauser, T.; Umari, P.; Vast, N.; Wu, X.; Baroni, S. Advanced capabilities for materials modelling with Quantum ESPRESSO*. J Phys Condens Matter*. **2017***. 29* (46). DOI:10.1088/1361-648X/aa8f79.

[11] Zeng, J.; Zhang, D.; Lu, D.; Mo, P.; Li, Z.; Chen, Y.; Rynik, M.; Huang, L.; Li, Z.; Shi, S.; Wang, Y.; Ye, H.; Tuo, P.; Yang, J.; Ding, Y.; Li, Y.; Tisi, D.; Zeng, Q.; Bao, H.; Xia, Y.; Huang, J.; Muraoka, K.; Wang, Y.; Chang, J.; Yuan, F.; Bore, S. L.; Cai, C.; Lin, Y.; Wang, B.; Xu, J.; Zhu, J. X.; Luo, C.; Zhang, Y.; Goodall, R. E. A.; Liang, W.; Singh, A. K.; Yao, S.; Zhang, J.; Wentzcovitch, R.; Han, J.; Liu, J.; Jia, W.; York, D. M.; Weinan, E. W.; Car, R; Zhang, L.; Wang, H. DeePMD-kit v2: A software package for deep potential models. *J Chem Phys.* **2023**. *159* (5). DOI:10.1063/5.0155600.

[12] Thompson, A. P.; Aktulga, H.M.; Berger, R.; Bolintineanu, D. S.; Brown, W. M.; Crozier, P. S.; In 't Veld, P. J.; Kohlmeyer, A.; Moore, S. G.; Nguyen, T. D.; Shan, R. Stevens, M. J.; Tranchida, J.; Trott, C.; Plimpton, S. J. LAMMPS - a flexible simulation tool for particle-based materials modeling at the atomic, meso, and continuum scales. *Comput. Phys. Commun.* **2022***, 271.* DOI: 10.1016/j.cpc.2021.108171

[13] Stukowski, A. Visualization and analysis of atomistic simulation data with OVITO-the Open Visualization Tool. *Modelling Simul. Mater. Sci. Eng.* **2010**, *18* (1)**.** DOI: 10.1088/0965-0393/18/1/015012

[14] Yang, G.; Li, L.; Lee, W.B.; Ng, M.C. Structure of graphene and its disorders: a review. *Sci Technol Adv Mater.* **2018**, *19* (1), 613-648. DOI: 10.1080/14686996.2018.1494493.